Am J Cancer Res 2022;12(2):521-536
www.ajcr.us /ISSN:2156-6976/ajcr0141018

Original Article

ONC206 has anti-tumorigenic effects in human ovarian cancer cells and in a transgenic mouse model of high-grade serous ovarian cancer

Katherine Tucker[1], Yajie Yin[1], Stuart-Allison Staley[1,3], Ziyi Zhao[1,2], Ziwei Fang[1,2], Yali Fan[1,2], Xin Zhang[1,2], Hongyan Suo[1,2], Wenchuan Sun[1], Varun Vijay Prabhu[4], Joshua E Allen[4], Chunxiao Zhou[1,5], Victoria L Bae-Jump[1,5]

[1]Division of Gynecologic Oncology, University of North Carolina at Chapel Hill, Chapel Hill, NC 27599, USA; [2]Department of Gynecologic Oncology, Beijing Obstetrics and Gynecology Hospital, Capital Medical University, Beijing 100025, China; [3]Rocky Mountain Gynecologic Oncology, Swedish Medical Center, Denver, CO 80113, USA; [4]Chimerix, Durham, NC 27713, USA; [5]Lineberger Comprehensive Cancer Center, University of North Carolina at Chapel Hill, Chapel Hill, NC 27599, USA

Received December 7, 2021; Accepted January 8, 2022; Epub February 15, 2022; Published February 28, 2022

Abstract: ONC206, a dopamine receptor D2 (DRD2) antagonist and imipridone, is a chemically modified derivative of ONC201. Recently, ONC206 and other imipridones were identified as activators of the mitochondrial protease ClpP, inducing downstream pathways that allow them to selectively target cancer cells. Clinical trials showed that ONC201, the first in class imipridone, was well tolerated and exhibited tumor regression in some solid tumors. Our goal was to evaluate the effect of ONC206 on cell proliferation and tumor growth in ovarian cancer cell lines and in a transgenic mouse model of high grade serous ovarian cancer (KpB model). ONC206 was more potent than ONC201 in inhibiting cell proliferation, as evidenced by a 10-fold decrease in IC50 for the SKOV3 and OVCAR5 cell lines. This was accompanied by the results that ONC206 significantly inhibited cellular proliferation, induced cell cycle G1 arrest and apoptosis, caused cellular stress, and inhibited adhesion and invasion *in vitro*. Treatment of obese and non-obese KpB mice with ONC206 elevated Bip and ClpP expression and reduced KI67, BCL-XL and DRD2 expression in the ovarian tumors. Our findings demonstrate that ONC206 has anti-tumorigenic effects in ovarian cancer as previously demonstrated by ONC201 but appears to be as well tolerated and more potent. Thus, ONC206 deserves further evaluation in clinical trials.

Keywords: ONC206, ovarian cancer, cell proliferation, apoptosis, adhesion/invasion

Introduction

Ovarian cancer (OC) is the second most common gynecologic malignancy and one of the deadliest cancers among women in the United States, with over 21,000 new cases estimated in 2021 [1]. Given the asymptomatic nature of early disease and the vague symptomatology if and when symptoms exist, women frequently present with advanced stage OC at the time of diagnosis. While the overall 5-year survival is close to 50%, the 5-year relative survival in women with distant metastatic disease is less than 30% [2, 3]. Based on the extent and distribution of disease at the time of diagnosis, patients undergo either primary debulking surgery followed by adjuvant chemotherapy or neoadjuvant chemotherapy followed by interval debulking surgery. The standard of care for neoadjuvant and adjuvant chemotherapy remains platinum/taxane doublet therapy [2, 4]. While the majority of patients will have no evidence of disease at the end of upfront treatment, 70-90% will recur [5]. There are a number of single agent, doublet and triplet combination chemotherapy regimens available in the setting of disease recurrence [6, 7]; however, given the cyclic nature of disease recurrence and the progressive shortening of the interval between disease free periods, new therapies are desperately needed.

ONC206 (Chimerix, Inc), a chemical derivative of imipridone ONC201, is part of the family of

compounds known as imipridones that share a tri-heterocyclic core structure and act as inducers of the integrated stress response (ISR) in tumor cells and TNF-related apoptosis-inducing ligand (TRAIL), a cytokine that selectively targets and kills tumor cells [8-10]. ONC201 is a dopamine receptor D2/3 (DRD2/3) antagonist and mitochondrial caseinolytic protease P (ClpP) agonist. Activation of TRAIL and ISR, increased expression of the DR5 death receptor, inhibition of AKT and ERK pathway activity, and targeting of mitochondrial metabolism are all inter-related downstream mechanisms that have been proposed [11, 12]. Early phase I results indicated that ONC201 is well tolerated and biologically active in the treatment of advanced solid tumors [8, 12]. Currently, ONC201 is being evaluated by multiple phase I/II clinical trials as an anti-tumor agent for various human cancers [13]. Recent literature demonstrates that ONC206 acts as a ClpP agonist with nanomolar potency and indicates comparable anti-tumor activity to ONC201 in diffuse intrinsic pontine glioma, neuroblastoma and glioblastoma [9, 11, 14, 15]. Our recent results showed that ONC206 exhibited anti-tumorigenic and anti-metastatic activity in uterine serous carcinoma (USC) *in vitro* and inhibited tumor growth in a transgenic mouse model of endometrial cancer under obese and lean conditions [16, 17].

Thus, our objective was to evaluate the potential anti-tumorigenic effects of ONC206 in OC cell lines and in a transgenic mouse model of high-grade serous OC. Our hypothesis was that ONC206 would demonstrate anti-tumorigenic effects in OC, with potentially greater potency than has been found for ONC201 [18]. Obesity is associated with worse outcomes in OC [19-21]. Our previous works have confirmed that obesity promotes ovarian tumor growth compared to lean mice and ONC201 has potentially increased anti-tumorigenic efficacy in obese versus lean mice with OC and endometrial cancer [22-25]. Therefore, we also examined the anti-tumorigenic efficacy of ONC206 in a transgenic mouse model of OC under obese and lean conditions.

Materials and methods

Cell culture and reagents

Two ovarian cancer cell lines, OVCAR5 and SKOV3, were used for cell proliferation assays and all other experiments. Both cell lines were maintained in DMEM/F12 medium with 10% fetal bovine serum (FBS). All media was supplemented with 100 U/ml of penicillin, 100 ug/ml of streptomycin, and L-glutamine 2 mM/mL. The cells were cultured in humidified 5% CO_2 at 37°C. ONC206 and ONC201 were obtained from Chimerix (Durham, NC). MTT (3-(5-dimethylthiazol-2-yl)-2,5-diphenyltetrazolium bromide), RNase A and RIPA buffer were purchased from Sigma (St. Louis, MO). All antibodies were obtained from Cell Signaling Technology (Beverly, MA). Enhanced chemiluminescence Western blotting detection reagents were purchased from Amersham (Arlington Heights, IL). All other chemicals were purchased from Sigma (St. Louis, MO).

Cell proliferation assays

The OVCAR5 and SKOV3 cells were plated and grown in 96-well plates at a concentration of 4.0×10^3 cells/well for 24 hours. The cells were then treated with various concentrations of ONC201 and ONC206 for a period of 72 hours. After the addition of MTT dye (5 mg/ml), the 96-well plates were incubated for an additional hour at 37°C. The MTT reaction was terminated through the addition of 100 uL of DMSO to each well. The plates were read by measuring absorption at 575 nm with a microplate reader (Tecan, Morrisville, NC). The effect of ONC206 was compared to the effect of ONC201 treated OVCAR5 and SKOV3 cells in the same manner as described above. Each experiment was performed at least three times to assess for consistency of results.

Annexin V assay

The effect of ONC206 on cell apoptosis was evaluated using the Annexin V-FITC Apoptosis Detection Kit (BioVision, Mountain View, CA). The cells were plated and grown in 6-well plates (2.5×10^5 cells/well) for 24 hours and then treated with varying concentrations of ONC206 for 30 to 36 hours. The cells were collected by a combination of 0.25% trypsin without ethylenediaminetetraacetic acid (EDTA) and 0.05% trypsin with EDTA (Gibco, Grand Island, NY). After washing with phosphate-buffered saline (PBS) solution, cells were resuspended in 100 ul of Annexin-V and propidium iodide (PI) dual-stain solution (0.1 ug of Annexin-V FITC and 1 ug of PI) for 15 minutes in the dark. Apoptotic cells were detected by Cellometer (Nexcelom

Bioscience, Lawrence, MA). The results were analyzed by FCS4 express software (Molecular Devices, Sunnyvale, CA). All experiments were performed at least three times to assess for consistency of response.

Cell cycle analysis

The effect of ONC206 on cell cycle progression was assessed using Cellometer. Cells were plated and grown at a density of 2.0×10^5 cells/well in 6-well plates for 24 hours and then treated with varying concentrations of ONC206 for 30 to 36 hours. Cells were collected by 0.05% trypsin, washed with PBS solution, fixed in a 90% methanol solution, and stored at -20°C until cell cycle analysis was performed. On the day of analysis, the cells were washed with PBS, centrifuged, and re-suspended in 50 ul RNase A solution (250 ug/ml) with 10 mM EDTA, followed by incubation for 30 minutes at 37°C. After incubation, 50 µl of propidium iodide (PI) staining solution (2 mg/ml PI, 0.1 mg/ml Azide and 0.05% Triton X-100) was added to each tube, and the cells were incubated for 10 minutes in the dark. The cells were then assessed by Cellometer. The results were analyzed using FCS4 express software. Each experiment was performed at least three times to assess for consistency of results.

Reactive oxygen species (ROS) assay

The Fluorimetric Intracellular Total ROS Activity Assay Kit (AAT Bioquest, Sunnyvale, CA) was used to detect alterations in the production of ROS caused by treatment with ONC206. Both OC cell lines (8.0×10^3 cells/well) were seeded into black 96-well plates. After 24 hours, the cells were treated with ONC206 and allowed to incubate for 16 hours at 37°C to induce ROS generation. DCFH-DA (20 µM) was then applied to the cells and allowed to incubate for 30 minutes. The fluorescence intensity was measured at an excitation wavelength of 485 nm and an emission wavelength of 530 nm using a microplate reader. All experiments were performed at least three times to assess for consistency of response.

Mitochondrial membrane potential assay

Mitochondrial membrane potential was analyzed using the specific fluorescent probes JC-1. The OVCAR5 and SKOV3 cells were plated and treated with different concentrations of ONC206 for 14 hours. The treated cells were then treated with 2 uM JC-1 for 30 minutes at 37°C. The microplate reader monitored the fluorescence intensity at the excitation/emission wavelength of 530/580 nm. Each experiment was repeated three times to assess for consistency of results.

Adhesion assay

Each well in a 96-well plate was coated with 100 ul laminin-1 (10 ug/ml) and incubated at 37°C for 1 hour. This fluid was then aspirated, and 200 ul blocking buffer was added to each well for 45 to 60 minutes at 37°C. The wells were then washed with PBS, and the plate was allowed to chill on ice. To each well, 1.2×10^4 cells were added with PBS and varying concentrations of ONC206. The plate was then allowed to incubate at 37°C for 2 hours. After this period, the medium was aspirated, and cells were fixed by adding 100 ul of 5% glutaraldehyde and incubating for 30 minutes at room temperature. Adhered cells were then washed with PBS and stained with 100 ul of 0.1% crystal violet for 30 minutes. The cells were then washed repeatedly with water, and 100 ul of 10% acetic acid was added to each well to solubilize the dye. After 5 minutes of shaking, the absorbance was measured at 575 nm using a microplate reader. Each experiment was repeated three times for consistency of response.

Invasion assay

The transwell migration assay system (Thermo Fisher Scientific, Waltham, MA) was used to determine invasion ability according to the manufacturer's protocol. OVCAR5 and SKOV3 cells were cultured with serum-free media for 12 to 14 hours. The cells (1×10^5) were then seeded in the transwell inserts of the wells in a 96-well plate. The lower chamber was added with regular media containing different concentrations of ONC206 for 4 hours. After washing lower chambers with PBS, 100 uL calcein AM solution was added to the lower chambers for 30 to 60 minutes. The lower chamber plate was measured by the microplate reader for reading fluorescence at excitation/emission (EX/EM) 485/520 nm. Each experiment was repeated three times.

Wound healing assay

In a 6-well plate, the OVCAR5 and SKOV3 cells were plated at 4.0×10^5 cells/well and incubated overnight. A uniform wound was created through the cell monolayer using a 20 ul pipette tip. The cells were washed and treated with different concentrations of ONC206 for 48 hours. Photos were taken at 24 and 48 hours after scratching, and the area of the scratch was analyzed with ImageJ software (National Institutes of Health, Bethesda, MD). Percent closure of the scratch was measured by comparing to control cells.

Cleaved caspase 3 assays

The OVCAR5 and SKOV3 cells were plated in 6-well plates (2.5×10^5 cells/well) for 24 hours and then the cells were treated with ONC206 at the indicated concentrations for 16 hours. Cells were washed with PBS and 200 ul lysis buffer was added into each well. Reaction buffer, containing caspase 3 substrates, was added to lysis buffer in a new black 96-well plate at 37°C for 20 to 30 minutes. The fluorescence intensity (EX/EM=465/540) for Caspase 3 activities were recorded using a microplate reader. These assays were repeated three times.

Measurement of vascular endothelial growth factor (VEGF) levels

To measure the VEGF concentration in OC cells, OVCAR5 and SKOV3 were incubated in 6-well plates for 24 hours. The cells were treated with different doses of ONC206 for 36 hours. Cell culture media was collected and then centrifuged at 2,000×g for 10 minutes to remove debris. Human VEGF ELISA Kit (Abcam, Waltham, MA) was used to determine the VEGF production following the protocol.

To measure VEGF concentration in the serum of mice after exposure to ONC206, 10 ul of serum were analyzed using a mouse VEGF ELISA kit (R&D Systems, Minneapolis, MN) according to the manufacturer's instructions. The optical density at 570 nM of each well was measured using a microplate reader.

Western immunoblotting

Following treatment of OVCAR5 and SKOV3 cells with varying concentrations of ONC206 for 6 to 36 hours, total protein was extracted from the cells of both cell lines using RIPA buffer. Equal amounts of protein were separated by gel electrophoresis and transferred onto a PVDF membrane. The membrane was blocked with 5% non-fat dry milk and then incubated with a 1:1000 dilution of primary antibody overnight at 4°C. The primary antibodies from Cell Signaling (Beverly, MA) used in this study were as follows: Mcl-1, Bcl-2, CDK4, CDK6, Calnexin, Ero1, and PERK, Snail, β-catenin, vimentin, VEGF. DRD2, DRD5, and DR5 antibodies were from Santa Cruz Biotechnology Inc. (Dallas, TX). The membrane was then washed and incubated with appropriate secondary peroxidase-conjugated antibody for 1 hour at room temperature after washing. Developing was used to detect antibody binding using an enhanced chemiluminescence detection buffer and the Bio-Rad Imaging System (Hercules, CA). After developing, the membranes were stripped or washed and re-probed using antibodies against α-tubulin or β-actin (Sigma, St. Louis, MO). Each experiment was repeated at least twice to assess for consistency of results.

K18-gT121$^{+/-}$p53$^{fl/fl}$Brca1$^{fl/fl}$ mouse model of serous OC

The K18-gT121$^{+/-}$p53$^{fl/fl}$Brca1$^{fl/fl}$ (KpB) mouse model is a high-grade serous OC mouse model that specifically and somatically deletes the tumor suppressor genes, BRCA1 and p53, and inactivates the retinoblastoma (Rb) proteins in adult ovarian surface epithelial cells following injection of Ad5-CMV-Cre (AdCre) directly into the one side of the ovarian bursa of 6-8 week old mice (KpB mouse model) [22, 26]. All mice were handled according to protocols approved by the University of North Carolina at Chapel Hill Institutional Animal Care and Use Committee (IACUC). The KpB female mice were fed a high-fat diet (HFD, 60% calories from fat) or a low-fat diet (LFD, 10% calories from fat, Research Diets) starting at 3 weeks of age. The mice were randomly divided into four groups (15 mice/group): HFD control, HFD+ONC206, LFD control and LFD+ONC206. When ovarian tumors reached 0.1-0.2 cm in diameter, the mice were treated with ONC206 (125 mg/kg, weekly, oral gavage) or placebo for 4 weeks. Tumor size was measured twice a week by palpation. Tumor volume was calculated using the following equation (width^2 × length)/2. All mice were euthanized after 4 weeks of ONC206 or vehicle treatment. Mice were weighed at sacri-

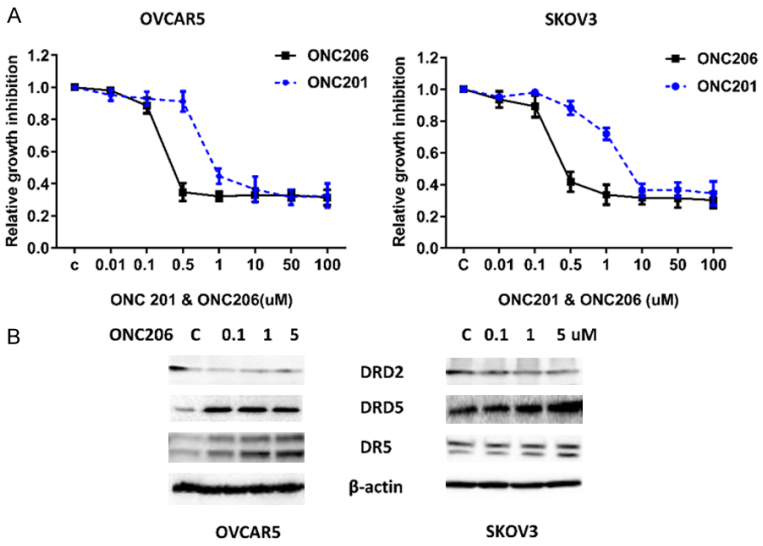

Figure 1. ONC206 inhibited cell viability. In 96 well plates, OVCAR5 and SKOV3 cells were treated with increasing concentrations of either ONC201 or ONC206 for 72 hours and subjected to the MTT assay. ONC201 and ONC206 significantly inhibited cell growth in a dose-dependent manner in all cell lines, although ONC206 was more potent with a lower IC50. Similar results were obtained from three independent experiments (A). Western immunoblotting was used to evaluate the effect of ONC206 on expression of DRD2, DRD5 and DR5 in the OVCAR5 and SKOV3 cells. ONC206 decreased the expression of DRD2 and increased the expression of DRD5 and DR5 in a dose-dependent manner in both cell lines after 24 hours of treatment (B).

fice, and blood samples were taken. Half of the ovarian tumor was snap-frozen and stored at -80°C, and the other half was fixed in 10% neutral-buffered formalin and paraffin embedded.

Immunohistochemistry (IHC)

Ovarian tumor slides (5 μm) were first incubated with protein block solution (Dako) for 1 hour and then with the primary antibodies for Ki-67, Bip, Clip, DRD2, BCL-XL and VEGF overnight in a cold room. The slides were then washed and incubated with appropriate secondary antibodies at room temperature for 1 hour. The slides were washed, and the specific staining was visualized using the Signal Stain Boost Immunohistochemical Detection Reagent (Cell Signaling Technology, Danvers, MA), according to the manufacturer's instructions. Individual slides were scanned using the Motic, and digital images were analyzed for target protein expression using ImagePro software (Vista, CA).

Statistical analysis

Data were presented as mean ± standard error of the mean. Statistical analysis of the differences between the groups was determined with the two-sided unpaired Student's t-test using GraphPad software (La Jolla, CA). A value of *P*-value of <0.05 was considered significant.

Results

ONC206 inhibits ovarian cancer cell proliferation more potently than ONC201

The effect of ONC206 and ONC201 on ovarian cancer cell proliferation was assessed by MTT assay. Two cell lines, OVCAR5 and SKOV3, were treated with varying concentrations (0.01 to 100 uM) of ONC201 or ONC206 for 72 hours. As shown in **Figure 1A**, ONC201 and ONC206 inhibited cell proliferation in both OC cell lines in a dose-dependent manner. For the cells treated with ONC206, the mean IC50 value for OVCAR5 and SKOV3 was 0.18 and 0.37 uM, respectively. For the cells treated with ONC201, the mean IC50 value for both OVCAR5 and SKOV3 was 1.78 and 3.52 uM. These results suggest that ONC206 effectively inhibits cell proliferation in OC cells as well as ONC201 and is more potent.

Next, we examined the effect of ONC206 on DRD2, DRD5, and death receptor 5 (DR5) in both cell lines. After OVCAR5 and SKOV3 cells were treated with ONC206 for 24 hours, western immunoblotting showed that ONC206 significantly increased expression of DR5 and DRD5 and dramatically decreased the expression of DRD2 in both cell lines (**Figure 1B**), suggesting that ONC206 inhibited cell proliferation through targeting DRD2 and DRD5 pathways and activating DR5 pathway in OC cells.

ONC206 induces apoptosis in ovarian cancer cells

The effect of ONC206 on apoptosis was evaluated using the Annexin V assay. This assay detects apoptotic cells by monitoring fluorescent-labeled Annexin V, which binds to phos-

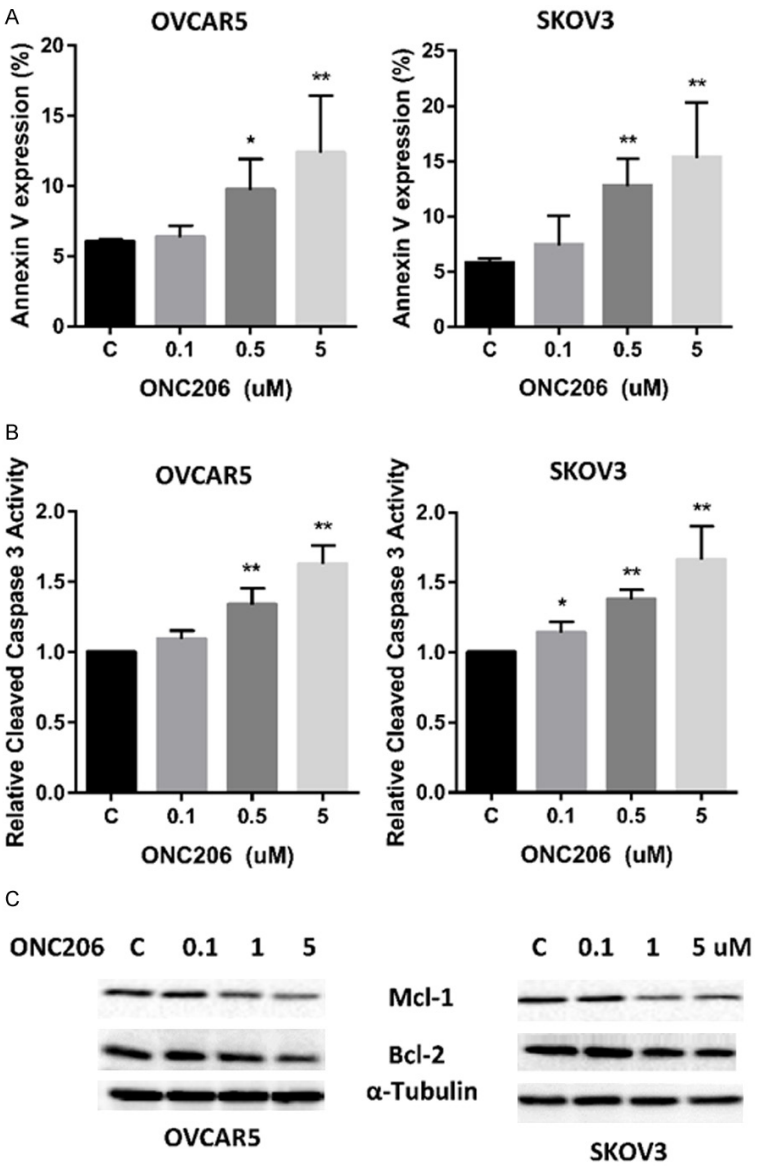

Figure 2. ONC206 induced apoptosis. OVCAR5 and SKOV3 cells were incubated for 30 to 36 hours with the indicated concentration of ONC206. Annexin V was analyzed by Cellometer. ONC206 caused increasing early apoptosis in a dose-dependent manner (A). Cleaved caspase 3 activity was assayed by ELISA assay. ONC206 induced the activity of the cleaved caspases 3 in both cell lines after treatment with ONC206 for 16 hours (B). Western immunoblotting showed ONC206 downregulated expression of Mcl-1 and Bcl-2 (C). The results are shown as the mean ± SD and are representative of three independent experiments. *P<0.05, **P<0.01.

phatidylserine externalized on the surface of the cell membrane and is representative of a distinct phenomenon of early apoptosis. OVCAR5 and SKOV3 were treated with ONC206 at varying concentrations (0.1-5 uM) for 30 to 36 hours. As shown in **Figure 2A**, the percentage of apoptotic cells increased in a dose-dependent manner in both cell lines (P<0.05). At a dose of 5 uM, ONC206 induced an average of 15.32% early apoptosis in SKOV3 and 12.26% early apoptosis in OVCAR5 cells. To evaluate whether mitochondrial apoptotic pathways were involved in apoptosis induced by ONC206, ELISA assays were applied to detect the activity of cleaved caspase 3 in OVCAR5 and SKOV3 cells after 16 hours of treatment. ONC206 significantly increased the level of cleaved caspase 3 in a dose-dependent manner. At a dose of 5 uM, ONC206 increased cleaved caspase 3 by 1.62 times in the OVCAR5 cells and 1.68 times in the SKOV3 cells (**Figure 2B**, P<0.05). Furthermore, Western immunoblotting showed that ONC206 down-regulated protein expression of apoptosis-related Mcl-1 (myeloid-cell leukemia 1) and Bcl-2 (B-cell lymphoma-2) (**Figure 2C**). These results suggest that ONC206 inhibits cell proliferation through induction of the mitochondrial apoptotic pathway in OC cells.

ONC206 induces cell cycle arrest in ovarian cancer cells

To evaluate the underlying mechanism of growth inhibition by ONC206, the cell cycle profile was analyzed after treating OVCAR5 and SKOV3 cell lines with varying doses (0.1-5 uM) of ONC206 for 30 to 36 hours. As illustrated in **Figure 3A**, ONC206 induced G0/G1 cell cycle arrest and reduced S phase and G2 phase in the both cell lines in a dose-dependent manner. In SKOV3, the number of cells in G1 cell cycle arrest increased from 50% in the control to 71.3% in the cells treated with 5 uM of ONC206 (P<0.05). The dose-dependent increase in cells in G1 cell

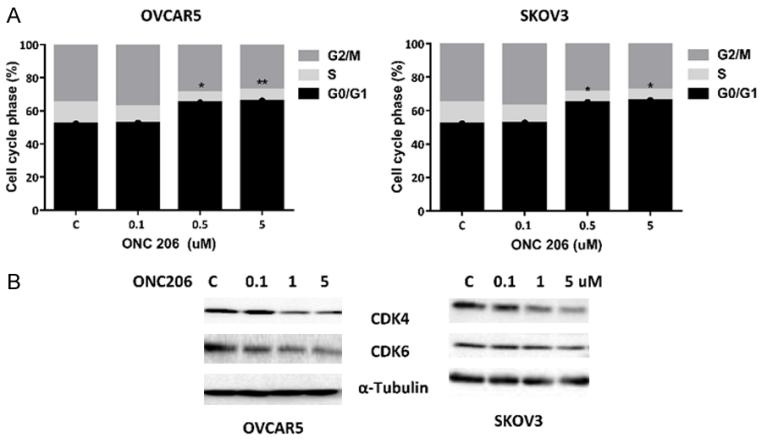

Figure 3. ONC206 induced cell cycle G1 arrest. The OVCAR5 and SKOV3 cells were incubated with increasing concentrations of ONC206 for 30 to 36 hours. Cell cycle progression was assessed by Cellometer. Cell cycle G1 arrest was found in both cell lines and increased in a dose-dependent manner (A). The cells were exposed to ONC206 prior to western immunoblotting for the detection CDK4 and CDK6. ONC206 decreased the expression of CDK4 and CDK6 (B). The results are shown are one of three independent experiments. *P<0.05, **P<0.01.

cycle arrest was noted at doses of 0.1 uM and 0.5 uM, at 57.8% and 66.8% respectively. In OVCAR5, the number of cells in G1 cell cycle arrest increased from 47.6% in the control to 64.6% in cells treated with 5 uM of ONC206 (P<0.05). The dose-dependent increase in cells in G1 cell cycle arrest was noted at doses of 0.1 uM and 0.5 uM, at 49.6% and 63.8% respectively. To further characterize ONC206's effect on cell cycle arrest, cell cycle-related proteins were analyzed in the two ONC206-treated cell lines. Western immunoblotting showed that ONC206 down-regulated the cell cycle-related proteins, CDK4 and CDK6 (**Figure 3B**). These data suggest that ONC206 induced inhibition of cell proliferation is also involved in cell cycle G1 arrest in OC cells.

ONC206 induces cell stress in ovarian cancer cells

Reactive oxygen species (ROS) have long been known to be a component of the cellular response to stress. Production of ROS by a diverse group of anti-cancer drugs has been closely related with the induction of apoptosis in cancers [27]. To investigate the involvement of oxidative stress in the anti-proliferative effect of ONC206, intracellular ROS levels were examined using the ROS fluorescence indicator DCFH-DA. After 16 hours of treatment, ONC206 (0.1-5 uM) significantly increased ROS production in a dose-dependent manner in the two ovarian cancer cell lines (**Figure 4A**, P<0.05). In SKOV3, ROS production increased 8%, 21% and 45% compared to the control after treatment with ONC206 doses of 0.1 uM, 0.5 uM and 10 uM, respectively (P<0.05). In OVCAR5, ROS production increased 10%, 23% and 31% compared to the control after ONC206 treatment with doses of 0.1 uM, 0.5 uM and 10 uM, respectively (P< 0.05). To further evaluate whether this increase in ROS is related to mitochondrial function, the JC-1 assay was used to detect alterations of mitochondrial membrane potential (ΔΨm). The results showed that ONC206 induced the loss of ΔΨm in a dose-dependent manner in both cell lines after 14 hours of treatment compared to control cells (**Figure 4B**, P<0.05). In addition, Western immunoblotting results showed that ONC206 significantly induced the protein expression of the endoplasmic reticulum (ER) stress-related proteins, PERK, Ero1, and calnexin, in both cell lines after 18 hours of treatment (**Figure 4C**). These results indicate that an increase in ROS production and ER stress might also be involved in the anti-proliferative effects of ONC206 in OC cells.

ONC206 decreases tumor growth in KpB mice under obese and non-obese conditions

To validate the anti-tumorigenic potential of ONC206 *in vivo*, we utilized the KpB serous ovarian cancer mouse model. The KpB mice were fed with either HFD and LFD and divided into four groups (n=15 mice/group). When tumors reached a size of 0.2 cm in diameter, the mice were treated with either ONC206 (125 mg/kg, Q week, IP) or placebo for 4 weeks. Tumor growth during treatment was monitored by palpation and caliper measurements twice a week. After 4 weeks of treatment, the mice were euthanized, and the ovarian tumors were removed, photographed, and weighed. ONC206 significantly inhibited tumor growth under obese and non-obese conditions (**Figure 5A**). ONC206 caused a significant decrease in tu-

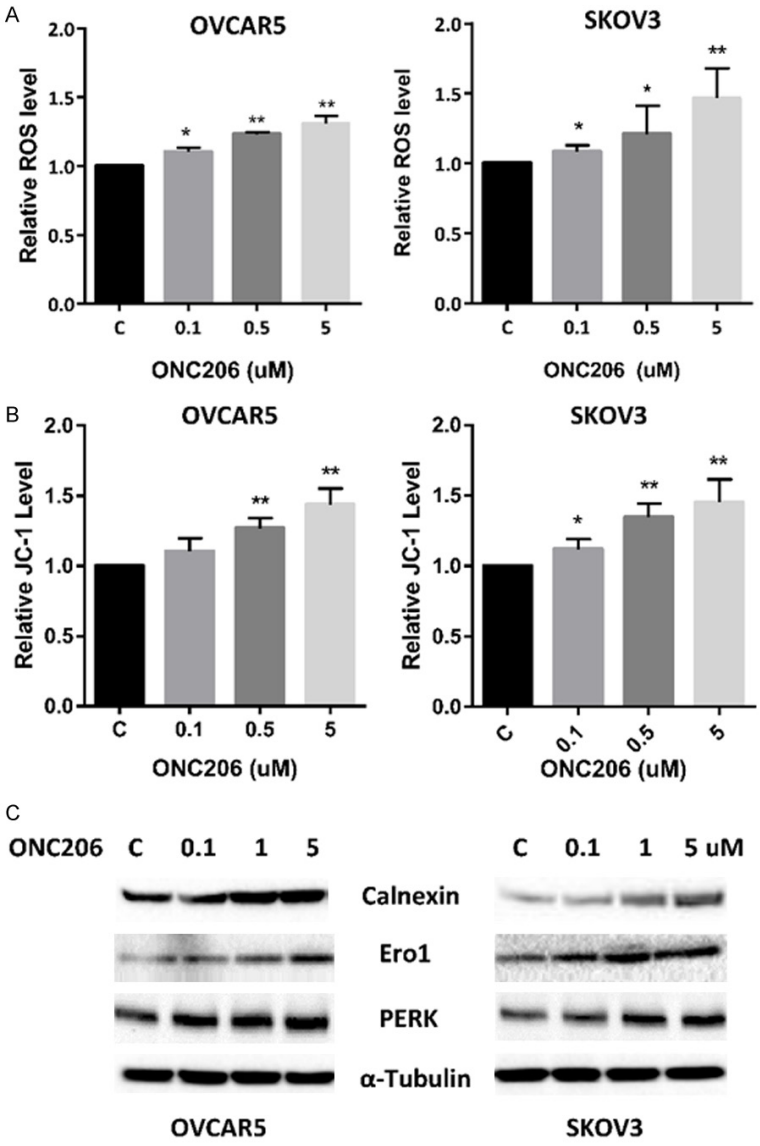

Figure 4. ONC206 induced cellular and endoplasmic reticulum stress. Cellular stress analysis was performed on the OVCAR5 and SKOV3 cells treated with different concentrations of ONC206. ROS and JC-1 products were measured by ELISA assays. ONC206 significantly increased the levels of ROS and decreased mitochondrial membrane potential in both cell lines compared to the control-treated cells (A and B). ONC206 increased the expression of cellular stress-related proteins including calnexin, Ero1, and PERK in both cell lines after treatment with ONC206 (C). The results are shown as the mean ± SD and are representative of three independent experiments. *P<0.05, **P<0.01.

mor weight (61.2%, P<0.01) among obese mice compared to the vehicle-treated controls. Similarly, treatment with ONC206 caused decreased tumor weight (49.6%, P<0.01) among non-obese mice (**Figure 5B**). During the treatment, the mice showed good toleration of ONC206 and maintained normal activities. Regular weekly measurements yielded no significant changes in blood glucose or body weight (data not shown).

To further confirm the antitumorigenic activity of ONC206 *in vivo*, the expression of Ki-67, BCL-XL, Bip, ClpP, and DRD2 in the ovarian tumor tissues was evaluated by immunohistochemistry (**Figure 5C**). Ki-67 and BCL-XL were significantly reduced following 4 weeks of ONC206 treatment in both obese and non-obese mice compared to the controls, whereas ONC206 increased the levels of Bip and ClpP in the treated mice. Consistent with our results *in vitro*, the expression of DRD2 was decreased in both obese and lean mice treated with ONC206 as compared to untreated mice. These results confirmed that ONC206 inhibits ovarian tumor growth *in vivo*.

ONC206 inhibits cell adhesion and invasion in ovarian cancer cells

Adhesion and invasion are important steps leading to metastasis in OC [28]. To determine the effect of ONC206 on adhesion and invasion of OC cells, an *in vitro* laminin adhesion assay, transwell invasion assay and wound healing assay were employed, respectively. Incubation of the OVCAR5 and SKOV3 cells with ONC206 at 0.1, 0.5 and 5 uM for 90 minutes in 96 well plate coated with laminin-1 showed a significant reduction in adhesion in both cells (**Figure 6A**, P<0.05). Treatment of both cells with ONC206 at dose of 5 uM significantly decreased cell invasion by 20.5% in OVCAR 5 and 22.1% in SKOV3, respectively, as determined by the transwell invasion assay (**Figure 6B**, P<0.05).

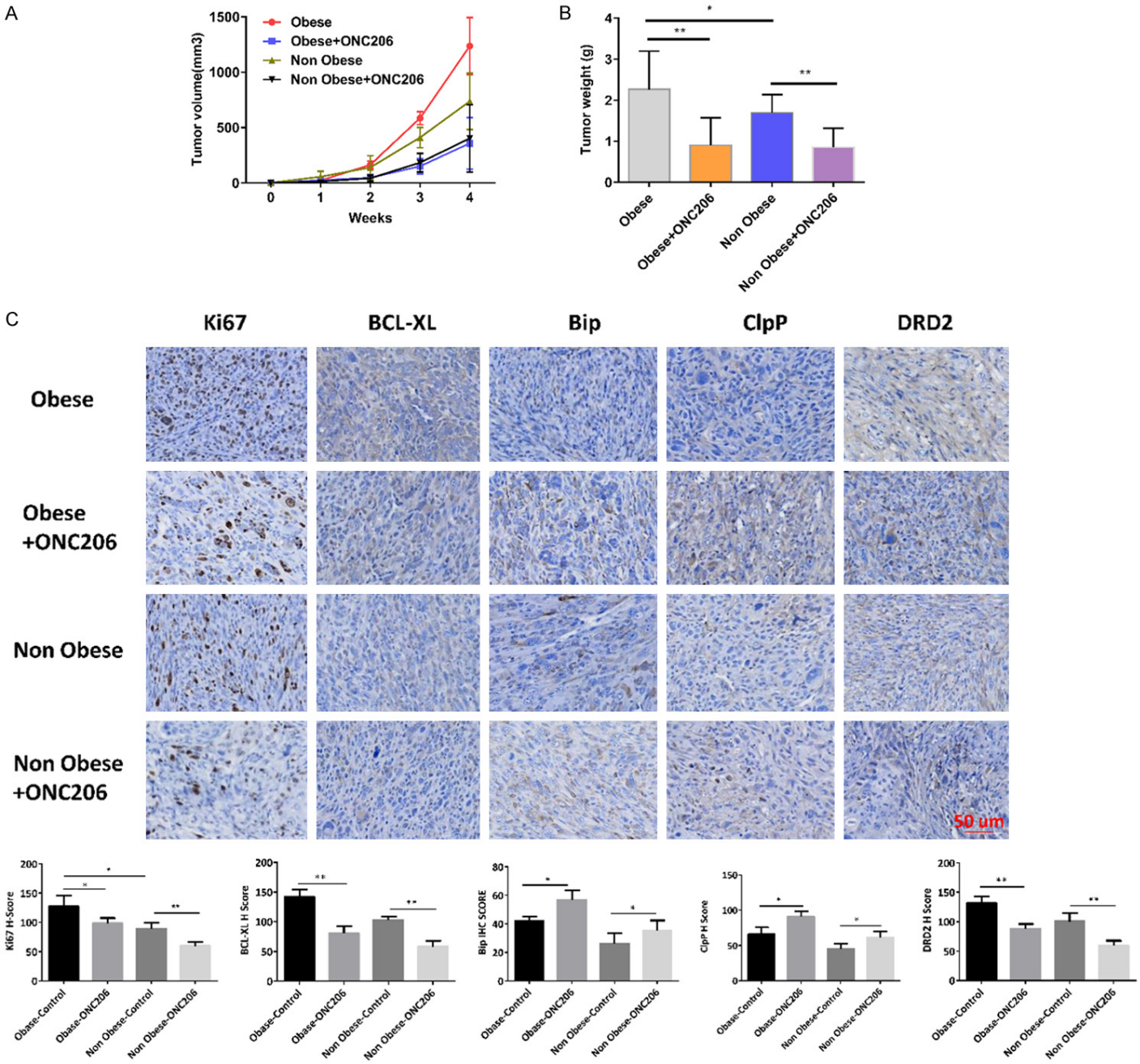
A
Tumor volume(mm3)
Weeks
Obese
Obese+ONC206
Non Obese
Non Obese+ONC206
B
Tumor weight (g)
C
Ki67
BCL-XL
Bip
ClpP
DRD2
Obese
Obese +ONC206
Non Obese
Non Obese +ONC206
50 um
Ki67 H-Score
BCL-XL H Score
Bip IHC SCORE
ClpP H Score
DRD2 H Score
Obase-Control
Obase-ONC206
Non Obese-Control
Non Obese-ONC206

Figure 5. ONC206 inhibited tumor growth in KpB mouse model of OC. Obese and lean KpB mice were treated with ONC206 (125 mg/kg, weekly) or vehicle for 4 weeks. Tumor volumes of ovarian tumors were measured weekly. The mean tumor volume was reduced in obese or lean mice treated with ONC206 (A). Tumor weight measurements of KpB mice were recorded at the time of sacrifice and were significantly reduced in both obese and lean KpB mice treated with ONC206 (B). The expression of Ki-67, BCL-XL, Bip, ClpP and DRD5 was assessed by immunohistochemistry analysis in the ovarian tumors following ONC206 treatment. ONC206 decreased the expression of Ki-67 and BCL-XL and increased the expression of Bip, ClpP and DRD5 in the ovarian tumor tissues under both obese and lean conditions (C). *P<0.05; **P<0.01.

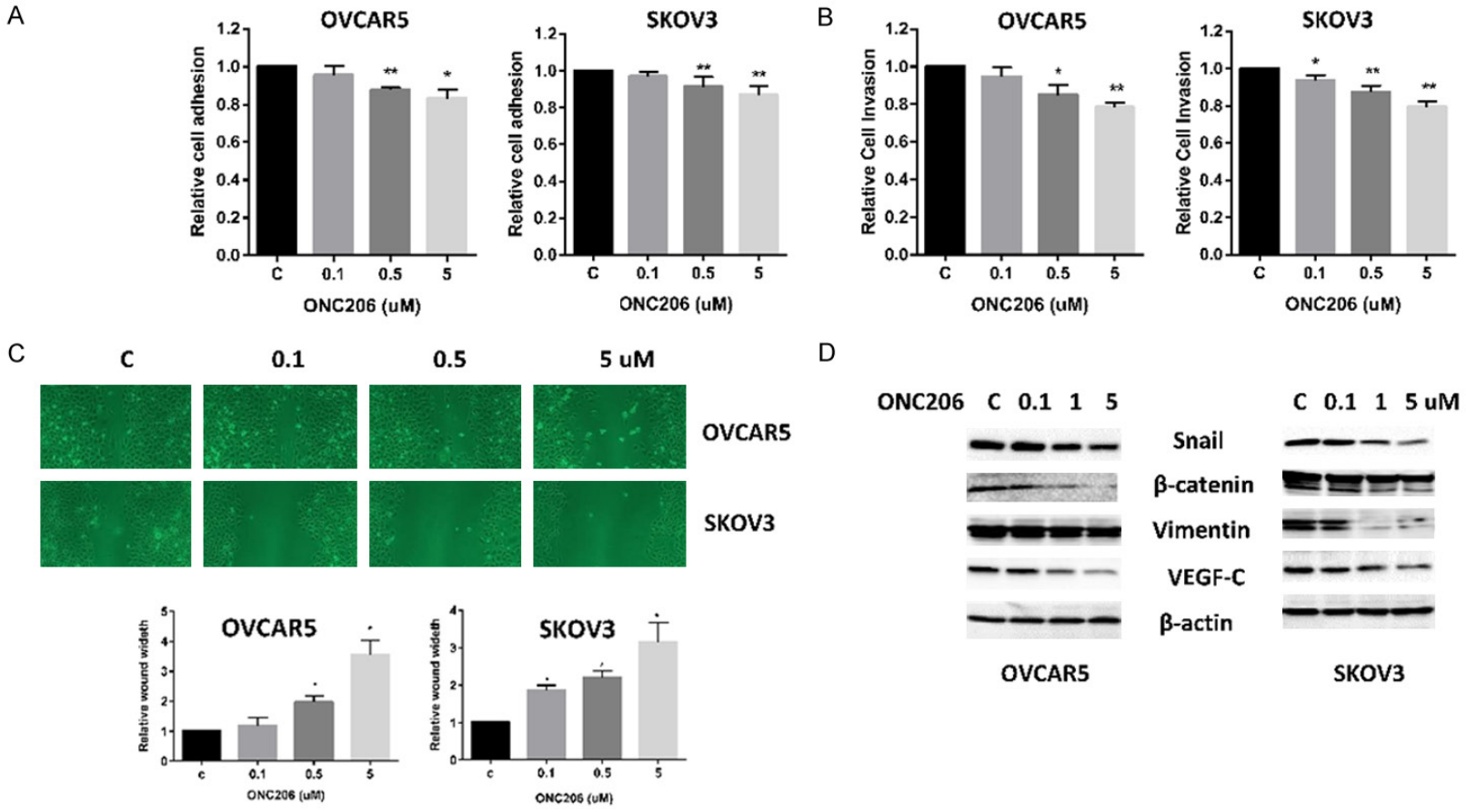

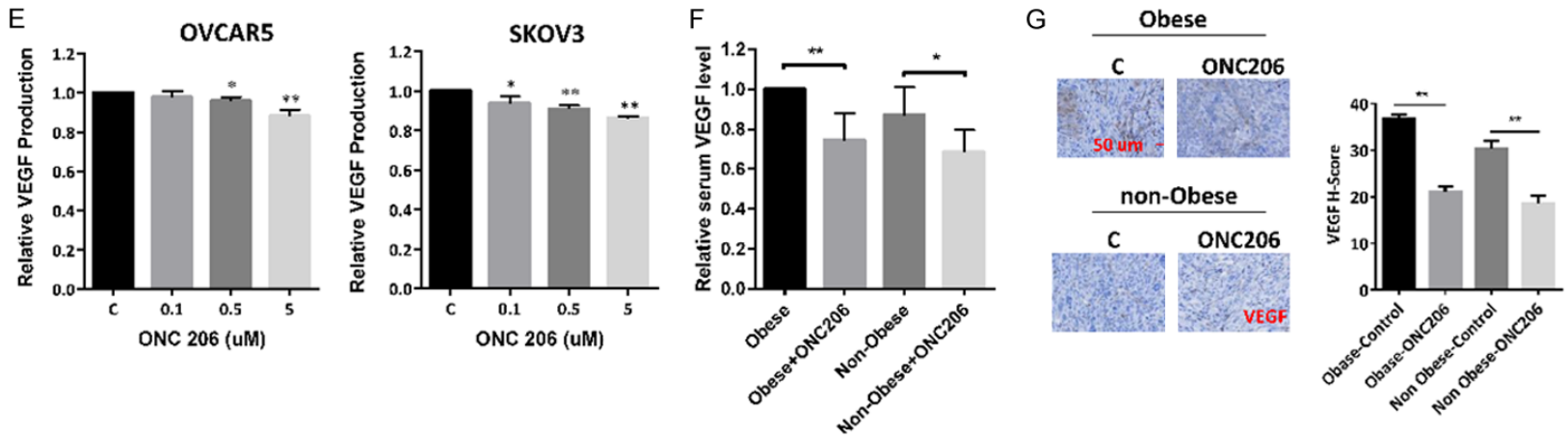

Figure 6. ONC206 inhibited adhesion and invasion, decreased VEGF production. The OVCAR5 and SKOV3 cells were treated with ONC206 at a range of doses from 0.1-5 μM. The laminin-1 assay was used to assess adhesion after 90 minutes of treatment with ONC206 (A). Invasion was examined by transwell assay after 4 hours of treatment with ONC206 (B). Migration was assessed by wound healing assay after treatment with ONC201 for 48 hours (C). Western immunoblotting found that ONC206 reduced the expression of snail, β-catenin, vimentin and VEGF in both cell lines (D). ELISA assay showed that ONC206 decreased VEGF production after treatment for 36 hours in both cell lines (E). The obese and lean KpB mice were treated with ONC206 for 4 weeks. Immunohistochemical results showed that ONC206 reduced VEGF expression in both obese and lean mice (F). Obesity was associated with increased serum VEGF production as compared to lean mice, and ONC206 reduced the production of VEGF in serum under both obese and lean conditions (G). $^{*}P<0.05$; $^{**}P<0.01$.

Inhibition of cell adhesion and invasion was occurred in a dose-dependent manner in both cell lines. Wound healing was examined at 24 and 48 hours, and the results showed that ONC206 slowed down cell migration back into the "wounded" area in both SKOV3 and OVCAR5 at 24 and 48 hours of treatment compared to control groups (**Figure 6C**, P<0.05). To further analyze the effect of ONC206 on angiogenesis and epithelial-to-mesenchymal transition (EMT) in OC cells, OVCAR5 and SKOV3 cells were treated with ONC206 for 24 hours. Western blotting results showed that ONC206 reduced the expression of Snail, β-catenin, Vimentin, and VEGF (**Figure 6D**). Using a VEGF ELISA assay, we determined the concentration of VEGF in cell culture media after treatment of ONC206 for 24 hours. ONC206 decreased the production of VEGF in a dose-dependent manner in both cells (**Figure 6E**, P<0.05).

To examine the effect of ONC206 on VEGF levels in serum and tumor tissue of KpB mice, serum VEGF production was determined by VEGF ELISA. Serum levels of VEGF were found to be decreased significantly by 25.6% in the obese mice (P<0.01) and 18.4% in the non-obese mice (P<0.05) treated with 4 weeks of ONC206 compared to control mice (**Figure 6F**). IHC results showed that expression of VEGF was slightly higher in obese than in non-obese mice. Treatment with ONC206 significantly reduced the protein expression of VEGF in ovarian tumor tissues under obese and non-obese conditions (**Figure 6G**, P<0.01). Overall, these results suggest that ONC206 has potential to inhibit adhesion and invasion in OC *in vitro* and *in vivo.*

Discussion

While high-grade serous OC remains highly responsive to platinum therapy in the frontline setting, its preponderance for development of platinum resistance necessitates the continued search for effective and well tolerated therapies to be used in the recurrent setting [29]. The improvement in our understanding of molecular and genetic changes implicated in OC pathogenesis has led to development of targeted therapies. Examples of this include the Federal Drug Association (FDA) approval of the anti-angiogenesis agent, Bevacizumab, and multiple Poly ADP-ribose polymerase (PARP) inhibitors for the treatment of select patients with OC [30]. Dopamine, a catecholamine neurotransmitter, is imperative in the regulation and processes of our central nervous system [31]. The dysfunction of the dopaminergic system, made up of a family of G protein-coupled receptors, is related to some neurologic diseases. Epidemiologic studies among patients with schizophrenia and Parkinson's disease, two diseases characterized by dopaminergic dysfunction, point to a possible relationship between dopamine receptors and the development of certain cancers [32-37]. While the risk of developing many cancers appears to be lower in patients with schizophrenia and Parkinson's disease, the studies examining these relationships often have heterogenous populations with many different cancer types included. High mRNA and protein expression of DRD2 has been observed in OCs, potentially linking this pathway to OC pathogenesis [38]. Furthermore, treatment with thioridazine, a DRD2 antagonist used in the treatment of schizophrenia, inhibited OC proliferation *in vitro* and *in vivo* [39].

ONC201 is a first-in-class small molecule selective DRD2 antagonist. Given the promising results of the first-in-human clinical trial of ONC201 in patients with refractory solid tumors [8], there are now multiple ongoing phase II clinical trials using ONC201 in select solid tumors, including platinum resistant and refractory OC. Our prior work showed that targeting DRD2 by ONC201 significantly inhibited cell proliferation and tumor growth in serous OC and uterus serous carcinoma cell lines and in a transgenic mouse model of high-grade serous OC under obese and lean conditions [24, 25, 40]. Recently, ONC206 entered a phase 1 trial as a single agent for the treatment of adults with recurrent and rare primary central nervous system neoplasms [13]. In the current study, we used ONC206, a more potent derivative of ONC201, to investigate its effects on cell growth, cellular stress, apoptosis, cell cycle progression, invasion/adhesion and tumor growth in OC cell lines and the KpB mouse model of high-grade serous OC. The results showed that ONC206 significantly reduced cell proliferation, caused cellular stress, induced cell cycle G1 arrest and apoptosis, and decreased invasion/adhesion in OC cells. Additionally, ONC206 inhibited ovarian tumor

growth along with decreasing DRD2, Ki67, VEGF and BCL-XL as well as increasing Bip and ClpP expression in ovarian tumors of both obese and lean KpB mice.

ONC206 was one of several imipridone analogues developed to capitalize on the anti-tumorigenic effects of its predecessor, with a similar low toxicity profile but distinct receptor pharmacology. The chemically modified and more potent ONC201 derivative, ONC206, showed promise as an active against central nervous system (CNS) tumors in preclinical work [9]. ONC206 is currently under investigation in Phase I studies in adult and pediatric patients with brain tumors. It exerts its effects through many of the same mechanisms as its parent-compound and has been shown to impair cell migration more robustly than ONC201 [41]. In our current study, we found that ONC206 decreased cell proliferation in OC cells with improved potency relative to ONC201 (i.e. 10 fold decrease in IC50 for ONC206 compared to ONC201) via similar mechanisms of action as we have previously shown for ONC201 [23, 40]. In addition, we recently compared the potential for cell growth inhibition of ONC201 and ONC206 in uterus serous carcinoma cells and found ONC206 was more effective in inhibiting cell proliferation compared to ONC201 [16, 40].

ONC201 exerts its anti-tumorigenic activity by ATF4/CHOP-mediated integrated stress response leading to TRAIL/DR5-induced apoptosis through inactivation of the AKT and ERK pathways [12, 42]. The inhibitory cell proliferation of ONC201 was associated with reduction of BCL-2 expression, activation of DR5 and induction of apoptosis independent of p53 via both a TRAIL-mediated apoptotic pathway and a mitochondrial apoptosis pathway in uterine serous cancer cells [40]. Importantly, ONC206 induced apoptosis and the expression of ER stress-related proteins including ATF4, PERK, and Bip; and inhibition of cellular stress by NAC partially negated the effects of ONC206 on cell proliferation in uterine serous cancer [16]. In this study, ONC206 induced caspase 3 activity, increased ROS and JC1 productions, decreased MCL-1 and BCL-2 expression, and caused an increase in PERK, Ero1 and Calnexin in OC cells. Treatment of ONC206 in KpB mice for 4 weeks significantly increased the expression of Bip and ClpP in the ovarian tumors. These results suggest that induction of cellular stress and apoptosis may be major mechanisms for the inhibition of cellular proliferation and tumor growth by ONC206 in OC.

Peritoneal dissemination is a unique and important method of metastasis that OC exploits, which involves epithelial-to-mesenchymal transition (EMT), a process in which epithelial cells lose their polarity and cell-to-cell adhesion to become more migratory [28, 43, 44]. Vascular endothelial growth factor (VEGF), a cytokine and regulator of angiogenesis, promotes angiogenesis and enhances vascular permeability resulting in the development of ascites and metastasis [45, 46]. Thioridazine, a DRD2 antagonist, was shown to inhibit VEGF-stimulated proliferation, invasion, and capillary-like structure tube formation in OC cells through the suppression of the αvβ3/FAK/mTOR pathway [47]. Recent results showed that the anticancer activity of ONC201 was dependent on transcriptional inhibition of VEGF Receptor 2 and RET in medullary thyroid cancer cells [48]. ONC201, in combination with bevacizumab, synergistically resulted in tumor regression or complete tumor ablation in colorectal cancer xenografts through independent mechanisms [49]. These results suggest that targeting VEGF by ONC201 or the combination of ONC201 and a VEGF inhibitor may represent a potent therapeutic approach in some types of cancer [48]. Our recent findings demonstrate that treatment with either ONC201 or ONC206 not only effectively inhibited the expression of VEGF but also reduced invasive ability through cellular stress-induced EMT process in uterus serous cancer cells [40]. Similar to our previous work with ONC201 and ONC206, this current study found that ONC206 reduced VEGF expression and inhibited adhesion and invasion of OC cells using the same EMT targets. More importantly, we also found that ONC206 decreased serum VEGF levels and VEGF expression in ovarian tumors under obese and lean conditions in a high-grade serous OC mouse model. Thus, the underlying mechanisms by which ONC206 inhibits invasion of OC cells may be dependent on the regulation of the EMT process and angiogenesis.

Mounting evidence points to obesity as a risk factor for OC and its association with a worse prognosis [19-21]. Given the fact that obesity can impact the efficacy of chemotherapy and

DRD2 signaling pathway in the brain has been implicated in obesity and metabolic dysfunction, we induced obesity by feeding a HFD (versus a LFD) to KpB mice, in order to observe the effectiveness of ONC206 treatment under obese and lean conditions. We found that obesity induced by a HFD significantly increased tumor weight and volume in the KpB mouse model of high grade serous OC, confirming previously described findings [22, 24]. ONC206 decreased tumor weight by 61.2% in obese mice and 49.6% in lean mice. Although no statistical significance was found in obese and lean mice, there seems to be a trend to potentially improve efficacy under obese conditions. In addition, treatment with ONC206 also increased expression of ClpP in the tumors of KpB mice, indicating that ONC206 may trigger cell death via activation of the ClpP pathway in OC.

In conclusion, we found that ONC206 inhibited proliferation of OC cells as well as induced cellular stress, cell cycle arrest and apoptosis. Importantly, ONC206 impaired OC cell adhesion and invasion, which are essential to promote metastatic spread of this disease. *In vivo*, ONC206 treatment caused a significant decrease in tumor weight and volume in a transgenic mouse model of high grade serous OC under both obese and lean conditions. Imipridones have emerged as a potential treatment among solid tumors. Our work points to an anti-tumorigenic effect of ONC206 for high grade serous OC *in vitro* and *in vivo* and confirms its higher potency compared to its parent compound, ONC201. Our study adds to the growing body of literature demonstrating the activity that imipridones have in the treatment of gynecologic cancers, and the promise ONC206 holds as an active agent against high grade serous OC, which will hopefully be evaluated in future clinical trials.

Acknowledgements

This work is supported by NIH/NCI-R37-CA226969.

Disclosure of conflict of interest

VVP and JEA are employees and stockholders of Oncoceutics/Chimerix. Oncoceutics/Chimerix provided ONC201 and ONC206 for these studies. No potential conflicts of interest were disclosed by the other authors.

Address correspondence to: Drs. Victoria L Bae-Jump and Chunxiao Zhou, Division of Gynecologic Oncology, University of North Carolina at Chapel Hill, Chapel Hill, NC 27599, USA. Tel: 919-843-4899; Fax: 919-966-2646; E-mail: victoria_baejump@med.unc.edu (VLBJ); Tel: 919-966-3270; E-mail: czhou@med.unc.edu (CXZ)

References

[1] Siegel RL, Miller KD, Fuchs HE and Jemal A. Cancer statistics, 2021. CA Cancer J Clin 2021; 71: 7-33.

[2] Trinidad CV, Tetlow AL, Bantis LE and Godwin AK. Reducing ovarian cancer mortality through early detection: approaches using circulating biomarkers. Cancer Prev Res (Phila) 2020; 13: 241-252.

[3] Moufarrij S, Dandapani M, Arthofer E, Gomez S, Srivastava A, Lopez-Acevedo M, Villagra A and Chiappinelli KB. Epigenetic therapy for ovarian cancer: promise and progress. Clin Epigenetics 2019; 11: 7.

[4] Ledermann JA. Front-line therapy of advanced ovarian cancer: new approaches. Ann Oncol 2017; 28 Suppl 8: viii46-viii50.

[5] Mullen MM, Kuroki LM and Thaker PH. Novel treatment options in platinum-sensitive recurrent ovarian cancer: a review. Gynecol Oncol 2019; 152: 416-425.

[6] Oronsky B, Ray CM, Spira AI, Trepel JB, Carter CA and Cottrill HM. A brief review of the management of platinum-resistant-platinum-refractory ovarian cancer. Med Oncol 2017; 34: 103.

[7] DiSilvestro P, Colombo N, Harter P, González-Martín A, Ray-Coquard I and Coleman RL. Maintenance treatment of newly diagnosed advanced ovarian cancer: time for a paradigm shift? Cancers (Basel) 2021; 13: 5756.

[8] Stein MN, Bertino JR, Kaufman HL, Mayer T, Moss R, Silk A, Chan N, Malhotra J, Rodriguez L, Aisner J, Aiken RD, Haffty BG, DiPaola RS, Saunders T, Zloza A, Damare S, Beckett Y, Yu B, Najmi S, Gabel C, Dickerson S, Zheng L, El-Deiry WS, Allen JE, Stogniew M, Oster W and Mehnert JM. First-in-human clinical trial of oral ONC201 in patients with refractory solid tumors. Clin Cancer Res 2017; 23: 4163-4169.

[9] Ishida CT, Zhang Y, Bianchetti E, Shu C, Nguyen TTT, Kleiner G, Sanchez-Quintero MJ, Quinzii CM, Westhoff MA, Karpel-Massler G, Prabhu VV, Allen JE and Siegelin MD. Metabolic reprogramming by Dual AKT/ERK inhibition through imipridones elicits unique vulnerabilities in glioblastoma. Clin Cancer Res 2018; 24: 5392-5406.

[10] Allen JE, Krigsfeld G, Mayes PA, Patel L, Dicker DT, Patel AS, Dolloff NG, Messaris E, Scata KA,

Wang W, Zhou JY, Wu GS and El-Deiry WS. Dual inactivation of Akt and ERK by TIC10 signals Foxo3a nuclear translocation, TRAIL gene induction, and potent antitumor effects. Sci Transl Med 2013; 5: 171ra17.

[11] Graves PR, Aponte-Collazo LJ, Fennell EMJ, Graves AC, Hale AE, Dicheva N, Herring LE, Gilbert TSK, East MP, McDonald IM, Lockett MR, Ashamalla H, Moorman NJ, Karanewsky DS, Iwanowicz EJ, Holmuhamedov E and Graves LM. Mitochondrial protease ClpP is a target for the anticancer compounds ONC201 and related analogues. ACS Chem Biol 2019; 14: 1020-1029.

[12] Prabhu VV, Morrow S, Rahman Kawakibi A, Zhou L, Ralff M, Ray J, Jhaveri A, Ferrarini I, Lee Y, Parker C, Zhang Y, Borsuk R, Chang WI, Honeyman JN, Tavora F, Carneiro B, Raufi A, Huntington K, Carlsen L, Louie A, Safran H, Seyhan AA, Tarapore RS, Schalop L, Stogniew M, Allen JE, Oster W and El-Deiry WS. ONC201 and imipridones: anti-cancer compounds with clinical efficacy. Neoplasia 2020; 22: 725-744.

[13] Bonner ER, Waszak SM, Grotzer MA, Mueller S and Nazarian J. Mechanisms of imipridones in targeting mitochondrial metabolism in cancer cells. Neuro Oncol 2021; 23: 542-556.

[14] Borsuk R, Zhou L, Chang WI, Zhang Y, Sharma A, Prabhu VV, Tapinos N, Lulla RR and El-Deiry WS. Potent preclinical sensitivity to imipridone-based combination therapies in oncohistone H3K27M-mutant diffuse intrinsic pontine glioma is associated with induction of the integrated stress response, TRAIL death receptor DR5, reduced ClpX and apoptosis. Am J Cancer Res 2021; 11: 4607-4623.

[15] El-Soussi S, Hanna R, Semaan H, Khater AR, Abdallah J, Abou-Kheir W and Abou-Antoun T. A novel therapeutic mechanism of imipridones ONC201/ONC206 in MYCN-amplified neuroblastoma cells via differential expression of tumorigenic proteins. Front Pediatr 2021; 9: 693145.

[16] Zhang Y, Huang Y, Yin Y, Fan Y, Sun W, Zhao X, Tucker K, Staley A, Paraghamian S, Hawkins G, Prabhu V, Allen JE, Zhou C and Bae-Jump V. ONC206, an imipridone derivative, induces cell death through activation of the integrated stress response in serous endometrial cancer in vitro. Front Oncol 2020; 10: 577141.

[17] Staley A, Tucker K, Yin Y, Zhang X, Fan Y, Zhang Y, Fang Z, Sun W, Suo H, Zhao X, Zhao Z, Prabhu VV, Allen JE, Zhou C and Bae-Jump VL. Highly potent dopamine receptor D2 antagonist ONC206 demonstrates anti-tumorigenic activity in endometrial cancer. Am J Cancer Res 2021; 11: 5374-5387.

[18] Rumman M, Buck S, Polin L, Dzinic S, Boerner J and Winer IS. ONC201 induces the unfolded protein response (UPR) in high- and low-grade ovarian carcinoma cell lines and leads to cell death regardless of platinum sensitivity. Cancer Med 2021; 10: 3373-3387.

[19] Delort L, Kwiatkowski F, Chalabi N, Satih S, Bignon YJ and Bernard-Gallon DJ. Central adiposity as a major risk factor of ovarian cancer. Anticancer Res 2009; 29: 5229-5234.

[20] Olsen CM, Green AC, Whiteman DC, Sadeghi S, Kolahdooz F and Webb PM. Obesity and the risk of epithelial ovarian cancer: a systematic review and meta-analysis. Eur J Cancer 2007; 43: 690-709.

[21] Pavelka JC, Brown RS, Karlan BY, Cass I, Leuchter RS, Lagasse LD and Li AJ. Effect of obesity on survival in epithelial ovarian cancer. Cancer 2006; 107: 1520-1524.

[22] Makowski L, Zhou C, Zhong Y, Kuan PF, Fan C, Sampey BP, Difurio M and Bae-Jump VL. Obesity increases tumor aggressiveness in a genetically engineered mouse model of serous ovarian cancer. Gynecol Oncol 2014; 133: 90-97.

[23] Pierce SR, Fang Z, Yin Y, West L, Asher M, Hao T, Zhang X, Tucker K, Staley A, Fan Y, Sun W, Moore DT, Xu C, Tsai YH, Parker J, Prabhu VV, Allen JE, Lee D, Zhou C and Bae-Jump V. Targeting dopamine receptor D2 as a novel therapeutic strategy in endometrial cancer. J Exp Clin Cancer Res 2021; 40: 61.

[24] Hawkins G, Fan Y, Fang Z, Huang Y, Sun W, Paraghamian S, Yin Y, Prabhu V, Allen J, Zhou C and Bae-Jump VL. ONC201 has anti-tumorigenic activity in obesity-driven epithelial ovarian cancer. Gynecol Oncol 2020; 159: 28-29.

[25] Fan Y, Wang J, Fang Z, Pierce SR, West L, Staley A, Tucker K, Yin Y, Sun W, Kong W, Prabhu V, Allen JE, Zhou C and Bae-Jump VL. Anti-tumor and anti-invasive effects of ONC201 on ovarian cancer cells and a transgenic mouse model of serous ovarian cancer. Social Science Electronic Publishing 2021.

[26] Szabova L, Yin C, Bupp S, Guerin TM, Schlomer JJ, Householder DB, Baran ML, Yi M, Song Y, Sun W, McDunn JE, Martin PL, Van Dyke T and Difilippantonio S. Perturbation of Rb, p53, and Brca1 or Brca2 cooperate in inducing metastatic serous epithelial ovarian cancer. Cancer Res 2012; 72: 4141-4153.

[27] Nakamura H and Takada K. Reactive oxygen species in cancer: current findings and future directions. Cancer Sci 2021; 112: 3945-3952.

[28] Yeung TL, Leung CS, Yip KP, Au Yeung CL, Wong ST and Mok SC. Cellular and molecular processes in ovarian cancer metastasis. A review in the theme: cell and molecular processes in cancer metastasis. Am J Physiol Cell Physiol 2015; 309: C444-456.

[29] Bast RC Jr, Hennessy B and Mills GB. The biology of ovarian cancer: new opportunities for translation. Nat Rev Cancer 2009; 9: 415-428.

[30] Wang Q, Peng H, Qi X, Wu M and Zhao X. Targeted therapies in gynecological cancers: a comprehensive review of clinical evidence. Signal Transduct Target Ther 2020; 5: 137.
[31] Vallone D, Picetti R and Borrelli E. Structure and function of dopamine receptors. Neurosci Biobehav Rev 2000; 24: 125-132.
[32] Ji J, Sundquist K, Ning Y, Kendler KS, Sundquist J and Chen X. Incidence of cancer in patients with schizophrenia and their first-degree relatives: a population-based study in Sweden. Schizophr Bull 2013; 39: 527-536.
[33] Chou FH, Tsai KY, Su CY and Lee CC. The incidence and relative risk factors for developing cancer among patients with schizophrenia: a nine-year follow-up study. Schizophr Res 2011; 129: 97-103.
[34] Li H, Li J, Yu X, Zheng H, Sun X, Lu Y, Zhang Y, Li C and Bi X. The incidence rate of cancer in patients with schizophrenia: a meta-analysis of cohort studies. Schizophr Res 2018; 195: 519-528.
[35] Wu Chou AI, Wang YC, Lin CL and Kao CH. Female schizophrenia patients and risk of breast cancer: a population-based cohort study. Schizophr Res 2017; 188: 165-171.
[36] Rugbjerg K, Friis S, Lassen CF, Ritz B and Olsen JH. Malignant melanoma, breast cancer and other cancers in patients with Parkinson's disease. Int J Cancer 2012; 131: 1904-1911.
[37] Driver JA, Logroscino G, Buring JE, Gaziano JM and Kurth T. A prospective cohort study of cancer incidence following the diagnosis of Parkinson's disease. Cancer Epidemiol Biomarkers Prev 2007; 16: 1260-1265.
[38] Moreno-Smith M, Lu C, Shahzad MM, Pena GN, Allen JK, Stone RL, Mangala LS, Han HD, Kim HS, Farley D, Berestein GL, Cole SW, Lutgendorf SK and Sood AK. Dopamine blocks stress-mediated ovarian carcinoma growth. Clin Cancer Res 2011; 17: 3649-3659.
[39] Yong M, Yu T, Tian S, Liu S, Xu J, Hu J and Hu L. DR2 blocker thioridazine: a promising drug for ovarian cancer therapy. Oncol Lett 2017; 14: 8171-8177.
[40] Fang Z, Wang J, Clark LH, Sun W, Yin Y, Kong W, Pierce SR, West L, Sullivan SA, Tran AQ, Prabhu VV, Zhou C and Bae-Jump V. ONC201 demonstrates anti-tumorigenic and anti-metastatic activity in uterine serous carcinoma in vitro. Am J Cancer Res 2018; 8: 1551-1563.
[41] Wagner J, Kline CL, Ralff MD, Lev A, Lulla A, Zhou L, Olson GL, Nallaganchu BR, Benes CH, Allen JE, Prabhu VV, Stogniew M, Oster W and El-Deiry WS. Preclinical evaluation of the imipridone family, analogs of clinical stage anti-cancer small molecule ONC201, reveals potent anti-cancer effects of ONC212. Cell Cycle 2017; 16: 1790-1799.
[42] Allen JE, Kline CL, Prabhu VV, Wagner J, Ishizawa J, Madhukar N, Lev A, Baumeister M, Zhou L, Lulla A, Stogniew M, Schalop L, Benes C, Kaufman HL, Pottorf RS, Nallaganchu BR, Olson GL, Al-Mulla F, Duvic M, Wu GS, Dicker DT, Talekar MK, Lim B, Elemento O, Oster W, Bertino J, Flaherty K, Wang ML, Borthakur G, Andreeff M, Stein M and El-Deiry WS. Discovery and clinical introduction of first-in-class imipridone ONC201. Oncotarget 2016; 7: 74380-74392.
[43] Nakanishi Y, Kodama J, Yoshinouchi M, Tokumo K, Kamimura S, Okuda H and Kudo T. The expression of vascular endothelial growth factor and transforming growth factor-beta associates with angiogenesis in epithelial ovarian cancer. Int J Gynecol Pathol 1997; 16: 256-262.
[44] Ramakrishnan S, Subramanian IV, Yokoyama Y and Geller M. Angiogenesis in normal and neoplastic ovaries. Angiogenesis 2005; 8: 169-182.
[45] Abu-Jawdeh GM, Faix JD, Niloff J, Tognazzi K, Manseau E, Dvorak HF and Brown LF. Strong expression of vascular permeability factor (vascular endothelial growth factor) and its receptors in ovarian borderline and malignant neoplasms. Lab Invest 1996; 74: 1105-1115.
[46] Olson TA, Mohanraj D, Carson LF and Ramakrishnan S. Vascular permeability factor gene expression in normal and neoplastic human ovaries. Cancer Res 1994; 54: 276-280.
[47] Byun HJ, Lee JH, Kim BR, Kang S, Dong SM, Park MS, Lee SH, Park SH and Rho SB. Anti-angiogenic effects of thioridazine involving the FAK-mTOR pathway. Microvasc Res 2012; 84: 227-234.
[48] Bagheri-Yarmand R, Dadu R, Ye L, Shiny Jebaraj Y, Martinez JA, Ma J, Tarapore RS, Allen JE, Sherman SI, Williams MD and Gagel RF. ONC201 shows potent anticancer activity against medullary thyroid cancer via transcriptional inhibition of RET, VEGFR2, and IGFBP2. Mol Cancer Ther 2021; 20: 665-675.
[49] Wagner J, Kline CL, Zhou L, Khazak V and El-Deiry WS. Anti-tumor effects of ONC201 in combination with VEGF-inhibitors significantly impacts colorectal cancer growth and survival in vivo through complementary non-overlapping mechanisms. J Exp Clin Cancer Res 2018; 37: 11.